frontiers in Earth Science

ORIGINAL RESEARCH
published: 27 July 2018
doi: 10.3389/feart.2018.00103

Sub-marine Continuation of Peat Deposits From a Coastal Peatland in the Southern Baltic Sea and its Holocene Development

Matthias Kreuzburg[1], Miriam Ibenthal[2], Manon Janssen[2], Gregor Rehder[1], Maren Voss[3], Michael Naumann[4] and Peter Feldens[5]**

[1] Marine Chemistry, Leibniz-Institute for Baltic Sea Research, Warnemünde, Germany, [2] Soil Physics, Faculty of Agricultural and Environmental Sciences, University of Rostock, Rostock, Germany, [3] Biological Oceanography, Leibniz-Institute for Baltic Sea Research, Warnemünde, Germany, [4] Physical Oceanography and Instrumentation, Leibniz-Institute for Baltic Sea Research, Warnemünde, Germany, [5] Marine Geology, Leibniz-Institute for Baltic Sea Research, Warnemünde, Germany

Coastal low-lying areas along the southern Baltic Sea provide good conditions for coastal peatland formation. At the beginning of the Holocene, the Littorina Sea transgression caused coastal flooding, submergence and erosion of ancient coastlines and former terrestrial material. The present Heiligensee and Hütelmoor peat deposits (located near Rostock in Northern Germany) were found to continue more than 90 m in front of the coastline based on on- and offshore sediment cores and geo-acoustic surveys. The seaward areal extent of the coastal peatland is estimated to be around 0.16–0.2 km^2. The offshore boundary of the former peatland roughly coincides with the offshore limit of a dynamic coast-parallel longshore bar, with peat deposits eroded seawards. While additional organic-rich layers were found further offshore below a small sand ridge system, no connection to the former peatlands can be established based on ^{14}C age and C/N ratios. The preserved submerged peat deposits with organic carbon contents of 37% in front of the coastal peatland Heiligensee and Hütelmoor was radiocarbon-dated to 6725 ± 87 and 7024 ± 73 cal yr BP, respectively, indicating an earlier onset of the peatland formation as presently published. The formation time of the peat layers reveals information about the local sea level rise. The local sea level curve derived from our ^{14}C-dated organic-rich layers is in general agreement to nearby sea level reconstructions (North Rügen and Fischland, Northern Germany), with differences explained by slightly varying local isostatic movements.

Keywords: coastal peatland, Holocene development of the southern Baltic Sea, shallow water hydroacoustic surveys, Heiligensee and Hütelmoor, submerged peatland, radiocarbon age dating of submerged peat deposits, peatland formation, sub-marine continuation of a coastal peatland

OPEN ACCESS

Edited by:
Elinor Andrén, Södertörn University, Sweden

Reviewed by:
Fabio Matano, Consiglio Nazionale Delle Ricerche (CNR), Italy
Ole Bennike, Geological Survey of Denmark and Greenland, Denmark

****Correspondence:***
Matthias Kreuzburg
matthias.kreuzburg@io-warnemuende.de
Peter Feldens
peter.feldens@io-warnemuende.de

Specialty section:
This article was submitted to Quaternary Science, Geomorphology and Paleoenvironment, a section of the journal Frontiers in Earth Science

Received: *30 April 2018*
Accepted: *05 July 2018*
Published: *27 July 2018*

Citation:
Kreuzburg M, Ibenthal M, Janssen M, Rehder G, Voss M, Naumann M and Feldens P (2018) Sub-marine Continuation of Peat Deposits From a Coastal Peatland in the Southern Baltic Sea and its Holocene Development. Front. Earth Sci. 6:103. doi: 10.3389/feart.2018.00103

INTRODUCTION

Shallow coastal areas and shorelines are important for social, economical, and scientific purposes, for example development of coastlines, land usage, and infrastructure, archeology, sediment dynamics, and biogeochemical fluxes (Small and Nicholls, 2003; Valiela, 2009; Wong et al., 2014). Soft coastlines around the globe increasingly suffer from adverse processes such as erosion, flooding and submergence. Sea level rise and climate change will increasingly stress and shape coastal urban living areas and ecosystems in the future (Vestergaard, 1997; Stigge et al., 2005; Thorne et al., 2007; Furmanczyk and Dudzinska-Nowak, 2009; Nicholls and Cazenave, 2010). In the Baltic Sea, present

shorelines were shaped during the Littorina Sea period since ∼8,000 cal yr BP (Björck, 1995; Lemke, 1998) following the last glacial maximum (LGM).

Ongoing coastal dynamic processes such as wave and current induced erosion, sediment transport and accumulation have influenced the evolution of coastlines immensely (Lehfeldt and Milbradt, 2000; Schlungbaum and Voigt, 2001; Harff et al., 2009). These processes have led to coastline displacement due to land-loss or land reclamation and therefore changed spatial extensions of coastal ecosystems and habitats. One of the most vulnerable coastal areas is low-lying coastal wetlands. These wetlands are highly endangered by sea water intrusion, erosion and submergence (Vestergaard, 1997; Nicholls and Cazenave, 2010; Wong et al., 2014). Along the Baltic Sea, about 1,800 km^2 of coastal wetland is influenced by saltwater intrusion (Sterr, 2008). Sea level rise is further expected to result in a loss of wetland areas in inland direction provided that accumulation of sediments is lower than erosion and the vertical growth rate is below that of sea level rise (Vestergaard, 1997; Lampe and Janke, 2004). During the post-glacial evolution of the southern Baltic Sea and the accompanying sea level rise (Lampe, 2005) sub-marine terraces of ancient shorelines developed (Kolp, 1990). With the onset of the Littorina transgression around 8000 calibrated years before present (cal yr BP) (Lampe, 2002; Reimann et al., 2011) the southern Baltic sea level rose rapidly to around 2 m below present sea level. Around 5,800 cal yr BP, the sea level stabilized and has remained largely stable in this local area since 4,000 cal yr BP. Where preserved, the age and position of basal peat deposits, as formed in former coastal wetlands, can be used to obtain information about past sea level (Milliman and Emery, 1968; Gehrels and Anderson, 2014).

The Holocene sea level rise in the Baltic Sea deviates strongly from the eustatic sea level rise and can vary widely locally. This was, and partly still is, caused by different effects of isostatic adjustment (Köster, 1961). The current isostatic movements result in a subsidence of the southern Baltic Sea coast by about 0.1–0.2 cm yr^{-1} (Lampe, 2005; Rosentau et al., 2007; Lampe et al., 2011), and an approximate relative sea level rise of 0.1–0.12 cm yr^{-1} (Dietrich and Liebsch, 2000) increasing the pressure caused by the eustatic sea level rise on the local coastal wetlands and also affecting the presence of bedforms in shallow waters.

In this study, we investigate the shallow offshore continuation of a coastal wetland at the southern coast of the Baltic Sea, using a combination of hydroacoustic methods, geologic surveys and physical and geochemical characterization of surface sediments and sediment cores. Our first objective is to determine the surface and subsurface structure offshore the wetland area and its former extension into the Baltic Sea. The second objective is to reconstruct the Holocene dynamic of the wetland formation and erosion.

STUDY SITE

The study site is a shallow coastal area (0–10 m depth) that adjoins an approximately 3 km long coastline of the nature reserve "Heiligensee und Hütelmoor" located northeast of Rostock-Warnemünde, northern Germany (**Figure 1**). The southwest-northeast striking coastline between the investigated area and the Fischland-Darß peninsula (**Figure 1**) is heavily exposed to the prevailing westerly wind conditions, mainly originating from low pressures crossing the northern Atlantic. Alongshore currents lead to sediment transport in a northeastern direction, accumulating along the barrier spit of the Fischland-Darß peninsula (Lampe et al., 2011). At the study site, a dune dike separates the coastline from the landside, which is a partly degraded peatland, extending 1.59 km in the north-south direction and 1.38 km in the east-west direction (Koebsch, 2013). To the east, the wetland is surrounded by the Rostocker Heide, a forest area with sandy soils >2 meter above mean sea level (m amsl). The formation onset of this low-lying (−0.1 to +0.7 m amsl) wetland is described to begin between 5,400 and 3,900 cal yr BP (Voigtländer et al., 1996; Bohne and Bohne, 2008). Following the glacial retreat, a post-glacial river delta (named the Ur-Recknitz) discharging into a glacial lake led to the partial erosion of glacial till and subsequent deposition of fine sand (Kolp, 1957). The constant rise of the sea level caused by the Littorina transgression, as well as the subsequent rise of the groundwater level resulted in organic material accumulation on top of the sands and led to the formation of the peatland (Dahms, 1991). Today, the onshore peat layer is up to 3 m thick (Voigtländer et al., 1996) behind the dune, and gradually thins out toward the surrounding forest. The peat consists of moderately to strongly decomposed Carex and Phragmites. Underneath, the peat layer is underlain by 3–10 m thick sediments of fine sands and glacial till. In the area surrounding Lake Heiligensee, lake sediments are found underneath the peat. The peatland was artificially drained by open ditches, with an intensive drainage starting in the 1970s, which caused a severe degradation of the upper peat horizons and subsidence of the soil surface. The peatland has been rewetted in 2010.

Within the last decades, the wetland has experienced multiple different ecological stages due to diverse anthropogenic influences (Voigtländer et al., 1996). Average coastal retreat rates between 1907 and 1971 were 114 cm yr^{-1} in the north (Rebentrost, 1973) and 20–25 cm yr^{-1} in the south of Lake Heiligensee (Kolp, 1957). To counter the continuing coastal erosion, an artificial dune dike was constructed in 1903 and rebuilt in 1963 (Miegel et al., 2016) to separate the low-lying areas from the Baltic Sea (Voigtländer et al., 1996; Bohne and Bohne, 2008). However, the area experienced several wash-over events, the latest in 1995, which required the reconstruction of the dune dike in 1996. With the aim of land renaturation, protection and maintenance of the dune system was abandoned in the year 2000. Since then, the coastline has been subjected to coastal erosion with coastal retreat rates of 120–210 cm yr^{-1} (Generalplan Küsten und Hochwasserschutz, Mecklenburg-Vorpommern). Estimation by Voigtländer et al. (1996) stated that since the onset of peatland formation, coastal erosion led to approximately 3 km of wetland-loss toward eastern direction. This results in outcropping peat-layers along the beach, which are then exposed to wave erosion along the seaward edge of the wetland following the abrasion of covering sand layers by storms.

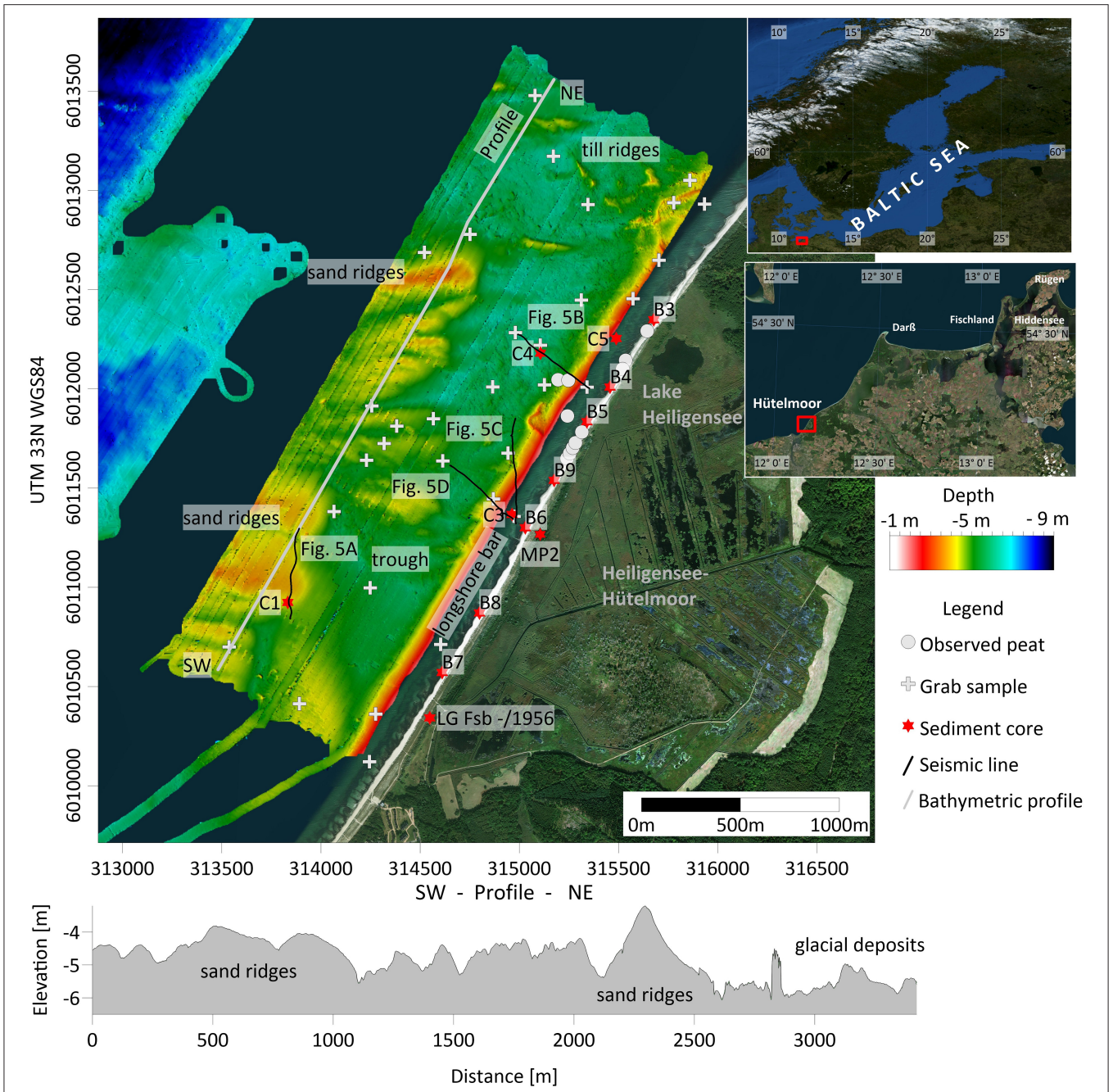

FIGURE 1 | (Top) Bathymetry and location of the study area along the southwestern Baltic Sea coast. White line parallel to the shore in SW-NE direction indicates the bathymetric cross section shown underneath. The positions of sediment cores (red stars) and grab samples (white crosses) are also indicated. The black lines show the locations of the seismic profiles. The longshore bar was identified from the parametric echosounder data (INNOMAR, see Methods). **(Bottom)** Bathymetric SW-NE transect at the upper shoreface indicating the distribution of the main geological units.

METHODS

Acquisition of Geophysical Data

Bathymetric and backscatter intensity data were collected with a Norbit iwbms multibeam echo sounder, which was pole-mounted on the research boat Klaashahn. Data in shallow waters (1.5–7 m) were recorded in June 2016 and July 2017. The Norbit iwbms uses an 80 kHz wide chirp signal centered at 400 kHz and an opening angle of 130–155°, set depending on water depth. Navigation data were acquired using an Applanix Surfmaster inertial navigation system utilizing the EGNOS correction. Total navigation accuracy is about 0.5 m both in the latitude and longitude direction. In addition to continuous sound velocity measurements at the multibeam transducer head, water

column sound velocity was measured using an SVP probe. The preparation of bathymetric data was completed using the Hypack (2016) software. Data processing included a quality control, the automatic, and manual removal of spikes, the correction of roll and pitch offsets, as well as the application of water column SVP profiles. Data were then gridded to a resolution of 0.5 m. Backscatter intensity data were processed using mbsystem (Caress and Chayes, 1995). A correction for the angular varied gain, including the multibeam residual beam pattern, was applied using mbbackangle. The backscatter data were passed through a gaussian low-pass filter to reduce speckle noise and gridded to a resolution of 0.5 m.

Seismic data were acquired using an INNOMAR standard parametric echo sounder during the June 2016 survey. In total, seismic data were acquired for the area covering a distance of 30 km. The system was pole-mounted on the Klaashahn research vessel. Data were recorded at frequencies of 8, 10, and 15 kHz, of which the 15 kHz frequency is shown in this study. A low pass swell filter was applied to remove heave artifacts caused by a malfunctioning motion sensor. However, due to the rapid movements of the small vessel, the wave impact could not be entirely removed. Two-way-travel time were converted to depths using a sound velocity of 1,480 m/s.

Ground Truthing

For seafloor ground truthing of the backscatter data, twelve 30 cm sediment cores were taken during scientific-diver missions and 20 surface sediment grab samples were taken from a boat. Deeper vertical ground truthing of the seismic data was achieved using 4 sediment cores (**Figure 1**) retrieved from maximum sediment depths of 280 cm with hand-pulling extraction tools from the BOREAS drilling platform (Lampe et al., 2009). The closed probe heads (STITZ) of 1 and 2 m, respectively were fitted with customized PVC liners of Ø46 mm for core extraction.

In total 7 sediment cores on land were taken with a percussion driller (Rammkernsonde). Open metal rods of Ø40 mm were used to sample sediment cores to a depth of −3.5 m below sea level (bsl). To assess the peat thickness in more detail, peat probings were conducted in the shallow coastal water. A Ø1 cm metal rod was pushed through the peat and stopped by the sand layer. All drilling and sampling locations were leveled with a real-time kinematic and differential GPS (Leica Viva Net-Rover).

Grain Size Distribution

Given the sandy composition of the analyzed sediments, no chemical pretreatment was performed. The grain size distribution of surface sediments (grab samples) was determined from sub-samples (∼150 g) of homogenized sediments. Dry sieving was conducted with DIN standard ISO 3310-1 sieves. Fractions <0,063 mm were lost during washing and were determined by weight difference compared to the total weight after washing and drying. Fractions >2 mm were retained. Automated sieving was conducted by a computer-controlled sieving tower (AS200) and a coupled Sartorius balance.

The grain size distribution of the sediment cores was determined by laser diffraction using an CILAS 1180, as not enough material for traditional sieving was available. Grain sizes larger than 1 mm cannot be measured with this method. To allow a comparison between the grain size distributions obtained with both methods, the first mode is used as the central statistical parameter. The mode is unaffected by removing the fine (mechanical sieving) or coarse (optical grain size distribution) sediment fraction, and can be used for bimodal sediments. All grain sizes are shown using the PHI scale, with PHI = – log2d, where d is the grain size in mm.

Geochemical Analyses and ^{14}C Dating

Organic carbon contents (C_{org}, after digestion with HCl) and stable isotope analyses of $\delta^{13}C$ of bulk material were performed on 2 onshore- and 3 offshore sediment cores using an infrared Elemental Analyzer Multi EA 2000 CS. Oven-dried samples were ground in an agate motor mill and homogenized. Splits of 10–20 mg powdered, homogenized sample were weighed in tin (C_{inorg}) and silver (C_{org}) containers (Nieuwenhuize et al., 1994). Stable isotope analyses of $\delta^{13}C$ was performed using an Isotope Ratio Mass Spectrometer (IRMS, Thermo Fisher Scientific), connected to an elemental analyzer via an open split interface. The $\delta^{13}C$ (‰) represents the isotope ratio of $^{13}C/^{12}C$ between the sample and a standard. The reference gas was ultra-pure CO_2 from a bottle calibrated against international standards (IAEA-C3, IAEA-C6, NBS 22) at the Leibniz-Institute for Baltic Sea Research (IOW). Calibration for carbon quantities was done with the reagent acetanilide. The lab internal standard was peptone (Merck) with a standard deviation of <0.2‰. AMS ^{14}C age control of plant material, shells, wood and bulk organic carbon dating (**Table 1**) was done by the commercial testing laboratory Beta Analytics (https://www.radiocarbon.com). Calibration of ^{14}C ages was done following Reimer et al. (2013).

RESULTS

Onshore

The general sediment sequence in a transect along the beach (**Figure 2**) shows a fine basin sand, at some spots followed by gyttja that presumably formed in former local depressions, and a peat layer on top. The peat is covered by marine medium to coarse, partly gravelly sands at the beach, and partly covered by dune sand further inland. In the north-eastern part of the transect, up to 2.5 m of silty to clayey sediments of gray-blueish to whitish color are found between the fine sands and the gyttja. The elevation of the peat surface along the transect decreases from NE to SW from 0.15 m bsl in core B5 to 2.84 m bsl in core B8. In addition, peat thickness tends to decrease in the same direction. The maximum peat thickness of 1.55 m (B9) and 1.4 m (B4) are found on top of gyttja. The minimum peat thickness of 0.1 m is found at B8. Further inland, the peat layer clearly extends southwards of core B7, indicating partial erosion of peat along the coastline. Additional peat probing conducted between B3 and B5 further seaward in shallow water depths (<0.5 m) indicate that the peat surface dips seawards. Sediment core MP2 (**Figure 1**) was retrieved near the position of B6 but further landward behind the dune dike. Here, the peat layer is found between depths of −0.7 and −3 m bsl with a 10 cm thick layer of gyttja below the base of the peat. The peat layer (and gyttja) at the beach (B6) was

TABLE 1 | Available age control ^{14}C in the study area. Age intervals are given at a 95.4% confidence interval.

Core ID	Core depth (cm)	Lat (N)	Long (E)	^{14}C age (yr BP)	cal yr BP	Material	C/N	$\delta^{13}C$ (‰)	C_{org} (%)
C1.1	190	54.212455	12.144969	8,040 ± 30	8,586 ± 256	Shell (Marine)	–	–	–
C1.2	190	54.212455	12.144969	4,430 ± 30	4,972 ± 137	Gyttja	11.97	−25.2	5.12
C3.1	150	54.216839	12.161998	5,900 ± 30	6,725 ± 87	Peat	36.4	−27.1	37.5
C3.2	165	54.216839	12.161998	6,160 ± 30	7,024 ± 73	Wood	15.2	−28.6	8.1
B9	305	54.218463	12.16515E	5,950 ± 30	6,769 ± 128	Gyttja	71.46	−30.5	50.25
B6.1	300	54.216265	12.163076	3,290 ± 30	3,516 ± 87	Peat	60.7	−28.08	51.06
B6.2	308	54.216265	12.163076	5,150 ± 30	5,918 ± 45	Gyttja	1.46	−27.92	19.83

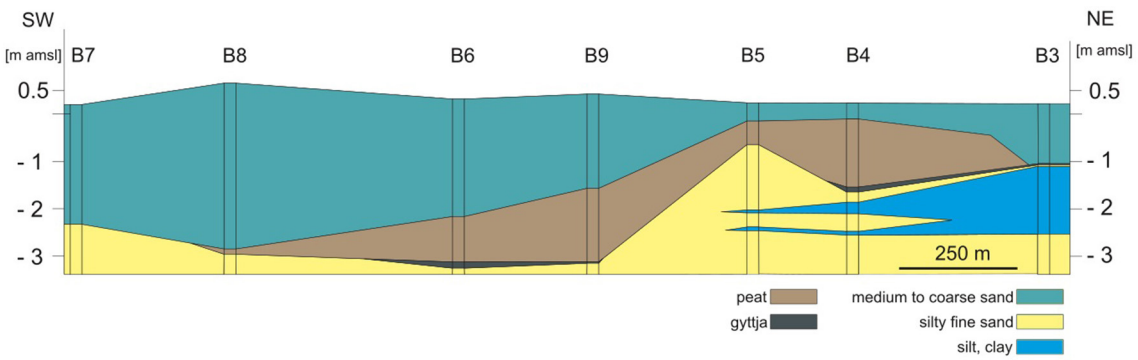

FIGURE 2 | Geological profile along the beach with drilling locations (B3–B9); sediment depth in meter above mean sea level (m amsl). Refer to **Figure 1** for coring locations.

also found to continue toward the hinterland behind the dune dike (MP2, **Figure 1**).

Offshore

Bathymetry

The bathymetric map (**Figure 1**) shows a series of sand ridges emerging seaward of a flat trough-like area. The SW/NE-elongated local trough extends roughly 1.2 km and is bound by nearshore sand bars in the east, and sand ridges in the southwest. The trough broadens in northern direction. Water depth in the broad northern part of the trough mostly exceeds ∼6 m. Here, numerous boulders and glacial till ridges, which have been observed during diver missions, are found. Several east-west to northwest-southeast oriented elevations of 450 m in length and up to 1.2 m in height are crossing the northern part of the trough. West and south-west of the trough, decreasing water depths are observed toward the sea. Here, a number of east-west oriented sand ridges 0.6–1.5 m in height, mostly 75–250 m in width, with one ridge reaching a width of 375 m, and up to 320 m observed length are located oblique (40–60°) to the coastline in water depths of 3–4 m. The maximum length of the ridges can be constrained to 1 km based on bathymetric data available further offshore (**Figure 1**). Generally, the ridges slope gently with angles mostly <0.5°. Although not all sand ridges follow the pattern, a slight asymmetry is observed, with wider and less inclined northern to north-western faces of the ridges (profile in **Figure 1**). In combination with the seismic data, a shore-parallel longshore bar can be identified that precedes the entire beach face. The longshore bar height is ∼1 m, while its width is 50–100 m.

Seafloor Composition

Backscatter mosaics ground-truthed with grab samples and short sediment cores allowed differentiation of three major facies types of seafloor in the study area (**Figure 3**): well sorted fine sand, medium sand with low gravel percentage, and poorly sorted coarse sand and gravel. The well-sorted fine sand is characterized by low backscatter intensities with a generally smooth and homogenous texture. It is mainly observed in the southern and south-western part of the study area in water depths of 4–6 m, forming the sand ridges in the south and south-west. The area covered by well-sorted fine sands may be further differentiated. While difficult to differentiate in acoustic data of the used frequency, available ground truthing data suggest a combined clay and silt fraction of ∼5% in the trough (**Figure 1**) separating the sand ridges and the beach face. The clay and silt fraction is absent within the sand ridges. In contrast, the sand ridges show a higher percentage of the medium to coarse sand fraction of ∼5%. Seafloor comprising medium sand with a low gravel percentage is characterized by medium backscatter intensities and is primarily observed along the runnels in-between the sand ridges, and fringing the boundaries of coarser sediment deposits. Seafloor composed of poorly sorted coarse sand and gravel (gravel content of up to 50%) is characterized by high backscatter intensities,

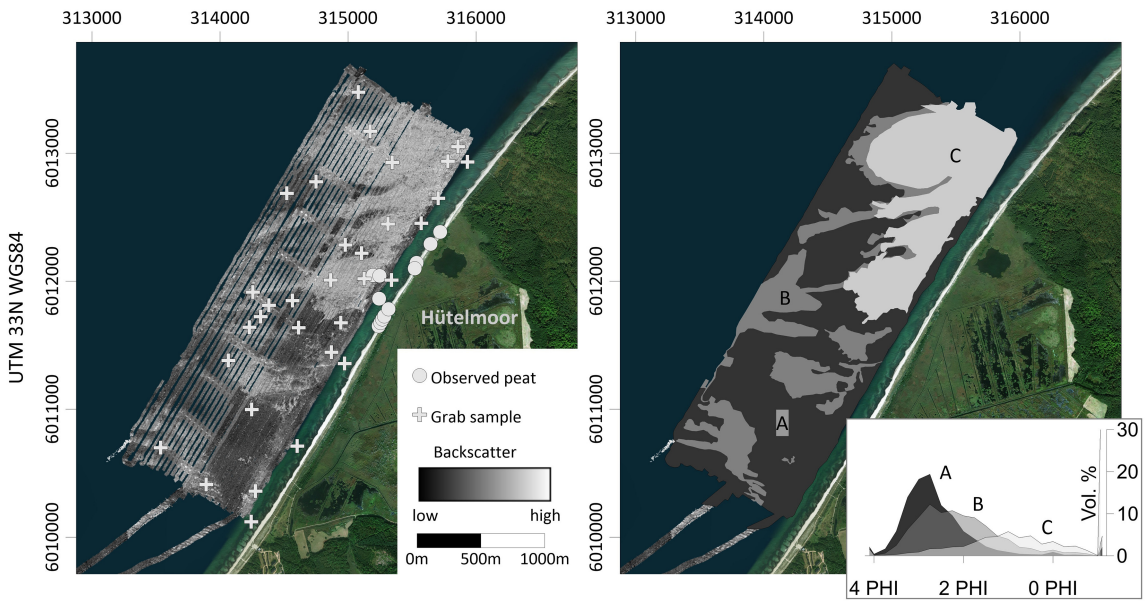

FIGURE 3 | (Left) Available backscatter data with grab samples for surficial ground truthing and near-coastal peat observations. **(Right)** Manual clustering of the backscatter data into three seafloor facies A–C. Representative grain size distributions for each facies are displayed, with A fine sand (black), B gravelly medium sand (gray), and C gravelly coarse sand (light gray). The insert in the **(Right)** panel indicates the grain size distribution (PHI-scale) in Vol %.

with numerous stones, boulders and uncovered glacial till. These deposits are observed in the north-eastern part of the study area (**Figure 3**).

Sediment Cores

Locations for sediment cores were selected based on thin seismic reflections, located parallel to the sediment surface at 3 m bsl and interpreted as the submerged extension of the peat sequence. Sediment core C1 was recovered in a water depth of 6.5 m (**Figure 4**, for location see **Figure 1**). At the base of the core from 280 to 248 cm depth, a sediment sequence composed of fine sand and scattered shell fragments was recovered, followed above by decimeter thick coarse and fine sand units, discontinued by layers of fine sand above. Following a sharp boundary, at 190 cm core depth two dark, 5- and 3 cm thick gyttja layers with shell fragments are separated by well-sorted fine sands. Two radiocarbon ages from the lower organic layer were determined from one sample (**Table 1**). The samples have different ages, with 8,586 ± 256 cal yr BP for marine shells fragments (Peringia ulva, Macoma Baltica) and 4,972 ± 137 cal yr BP for the bulk organic sediments (C_{org} 5.12%, $\delta^{13}C$ −25.2‰, C/N-ratio 11.97).

Sediment core C3 (**Figure 4**) has a total length of 197 cm, and was recovered in a water depth of 1.8 m. The lowest unit (171–197 cm) is mostly composed of fine sand featuring dark layers with C_{org} of 0.4%, $\delta^{13}C$ of −27.2‰ and C/N-ratios of 11.6. It is followed by a gyttja layer (C_{org} 8.1%, $\delta^{13}C$ −28.6‰, C/N-ratios 15.2) containing wooden fragments, which were dated to 7,024 ± 73 cal yr BP (C3.2) and a decimeter thick peat layer at 146–160 cm depth. Peat material (C3.1) has been dated to 6,725 ± 87 cal yr. Organic carbon contents of 36.9 and 37.5% (C_{org}), stable isotopic signatures of ($\delta^{13}C$) −28.9 and −27.1‰ and C/N ratios of 21.3 and 36.4 were measured in this peat layer. The peat layer itself is a horizon of a pure freshwater habitat representing a former preserved land surface. Separated by an erosional boundary, sediments above the peat are mostly composed of fine to medium marine sands with little change in grain size distribution.

Sediment core C4, with a total length of 120 cm, was retrieved in a water depth of 5.3 m. The bottom part (113–120 cm) is composed of glacial till. Sediments above the till, separated by a sharp boundary, alternate between fine and medium sands. Surface sediments (4–12 cm) are composed of dark coarse sand including coarse gravel of 2–3 cm diameter, sharply followed by dark fine sands. Sediment core C5 was retrieved in a water depth of 1 m and has a total length of 117 cm. The bottom sediment in C5 is composed of medium sand containing fine gravels with low sphericity. Above a diffuse transition, it is followed by two distinct layers of minerogenic lake sediments at 110–93 and 88–62 cm that are separated by a well-sorted fine sand layer of ∼5 cm thickness. Above, a coarsening upwards trend of medium to coarse sands prevails. At 38 cm a black layer of ∼3 mm thickness with C_{org} of 1.22%, $\delta^{13}C$ of −24.36‰, and C/N of 10.66 is observed.

Subsurface Structure

Subsurface information is derived from seismic reflection data (**Figure 5**, for location see **Figure 1**) and ground truthing by sediment cores of various lengths. Glacial till that commonly forms the acoustic basement for high-frequency seismic surveys in the Baltic Sea, forms the substratum of the observed stratigraphy. The glacial till is generally dipping from North to South. In addition, its top is slightly inclined toward the offshore

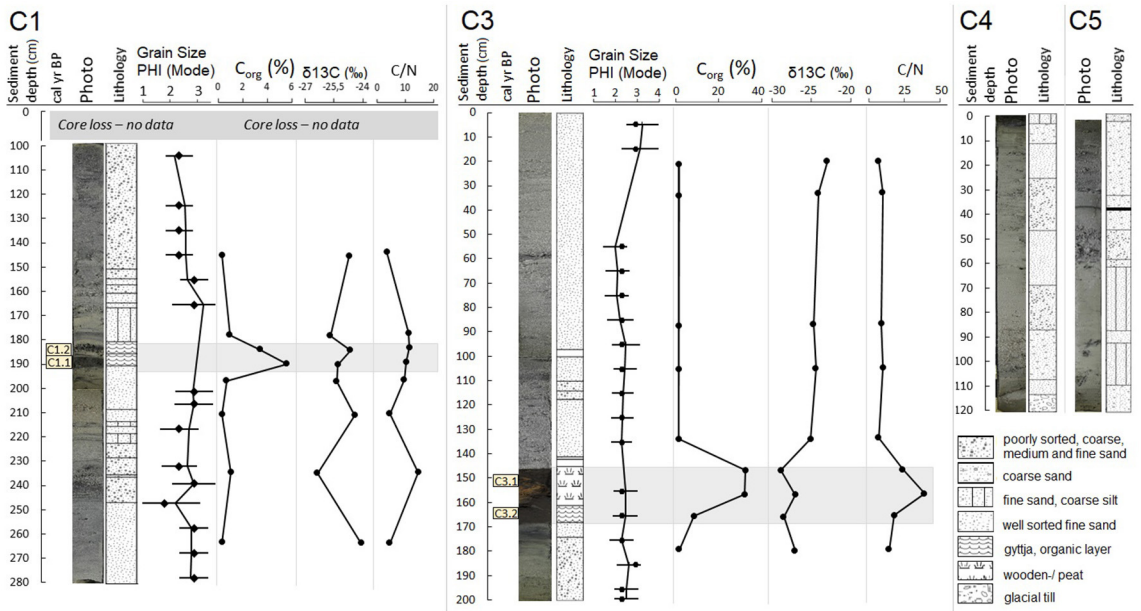

FIGURE 4 | Sediment depths (cm), radiocarbon age-dating, photographs, lithology, grain size distribution, organic carbon content (%), isotope ratio $\delta^{13}C$ (‰), Carbon/Nitrogen ratios (C/N) of the 4 offshore sediment cores (C1, C3, C4, C5) retrieved from the study site.

direction and is marked by steep irregularities, corresponding to outcropping till ridges observed in the bathymetric data. The burial depth of the till surface controls the accommodation space available for the overlying sediments. Acoustically homogeneous to transparent material (**Figures 5A–D**, labeled with medium sand) partly fills the irregularities. Where these materials outcrop at the seafloor, medium sand with low gravel percentage is retrieved in grab samples (**Figure 5B**). Layered sedimentary units (marked with H in **Figures 5A–D**) thin as till deposits emerge in the north of the research area. Based on ground truthing with sediment cores C1 and C3, the layered sediments are of Holocene age. They are characterized by high amplitudes and frequently show internal reflectors indicating different layers of sediment. In several locations, a chaotic and disturbed appearance of the Holocene deposits prevails, and individual reflectors cannot be followed. The Holocene sequence includes organic sediments and peat that have been retrieved in sediment cores C1 and C3. At the exact location of the sediment cores, the peat layer is difficult to recognize in the seismic data. Thin reflections located roughly parallel to the sediment surface at a depth of ∼3 m bsl (**Figures 5B–D**) are interpreted as corresponding to the peat sequence observed in the cores at the same depth. The peat layer continues with decreased reflection intensities beneath the longshore sand bar observed in bathymetric data, where it terminates unconformably against its seaward base (**Figures 5B–D**). Its continuation landwards of the coring position cannot be reliably determined due to the shallow multiple. In the seismic data, the longshore sand bar shows faintly visible internal, offshore-directed lamination. It has medium to low acoustic transparency, and a maximum observed thickness of ∼1.5 m. In the western and south-western part of the investigated area, sand ridges composed of fine sand (**Figure 5A**) unconformably overlie the layered deposits beneath. The sand ridges are characterized by a homogeneous, transparent signature with hardly any internal reflections. They reach an observed thickness of ∼1 m at maximum. Showing the same acoustic characteristics but located further north, isolated lenses of fine sand with a thickness of <1 m are deposited on top of the medium sand (**Figure 5B**). Several profiles in the near-coastal-zone of the central study area are cross-cutting a shore-parallel sand bar.

DISCUSSION

Geomorphological Setting

The combination of high resolution hydro-acoustics, subsurface information and sediment composition analyses confirms large heterogeneities between the northern and the southern shoreline as well as the offshore sand ridge area. Well- sorted fine sands prevailingly cover the southern trough area and form the sand ridges, medium sands with low gravel percentage separate the sand ridges and the northern plain area where glacial deposits are located close to the seafloor surface. In contrast, increasing sedimentation of medium to fine sand results in decreasing water depths and sheltered environments toward the south, indicated by internal lamination of Holocene deposits (**Figures 5B–D**) in the seismic data.

The sand ridges are a prominent geomorphological feature in this nearshore study site. Shoreface connected sand ridges are widespread on continental shelves, and are best described in the eastern Atlantic and in the Dutch and German part of the North Sea (van de Meene and van Rijn, 2000; Zeiler et al., 2008). Sand

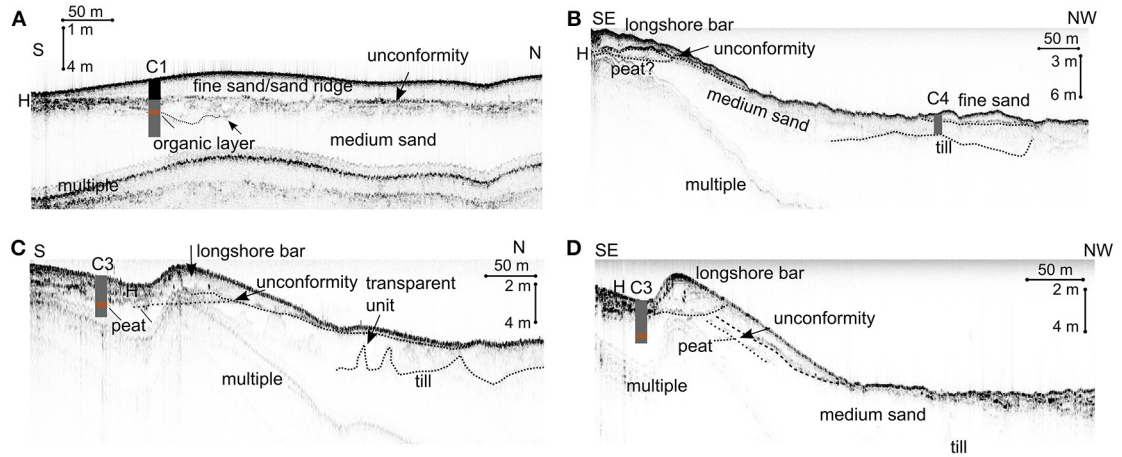

FIGURE 5 | Seismic data of profiles **(A–D)**. Sediment cores to prove the ground truthing are indicated. The position of core C3 was extrapolated to the nearest shot points of seismic lines **(C,D)**. The distance to line **(C)** is 25 m, and the distance to line **(D)** is 15 m. Refer to **Figure 1**. for location of the seismic lines.

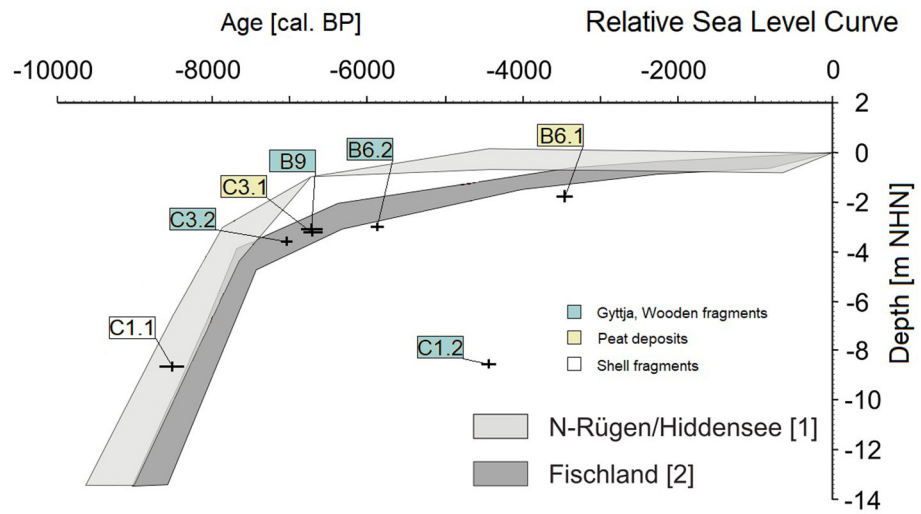

FIGURE 6 | Local Holocene sea level curve based on Lampe et al. (2010) with age/depth relationships obtained in this study.

ridges are formed both by tidal currents (negligible in the Baltic Sea) as well as by wind/storm generated longshore currents, and they can persist for several thousand years (Snedden and Dalrymple, 1999). However, no reports of shoreface connected sand ridges in the southern Baltic Sea exist to our knowledge. A main reason for the local scarcity of sand ridges is the heterogeneous and patchy sediment composition in the Baltic Sea compared to other shelf regions causing sediment-starved conditions (Schwarzer, 2010; Feldens et al., 2015). Thus, the Baltic Sea lacks sufficient sand supply for the formation of sand ridges in most regions. Still, the sand ridges observed offshore the Hütelmoor is interpreted as a small sand ridge field. The ridges downdrift tip is oriented toward the coast, in agreement with dominant SW-NE directed longshore currents. The variable length-to-width ratio (∼ 2 to 10), which is lower here by the Hütelmoor than in comparable nearshore ridges (Pendleton et al., 2017), low height (Nnafie et al., 2014), and shallow base may indicate a frequent reworking of the fine sand ridges by background wave action, while formation of the ridges requires intense storm activity (Swift et al., 1978). The time of formation of the sand ridges offshore the Hütelmoor can be constrained by the available ^{14}C date within core C1 and the seismic data. Since the base of the sand ridges forms an unconformity to the material of core C1 (**Figure 5A**), they have to be formed subsequently to the deposition of the youngest dated material below at 3,582–3,450 cal yr BP at a time when the Baltic Sea sea level reached its present value and was approximately nearly stable (**Figure 6**).

The entire beach area is preceded by a longshore bar (**Figure 1**) consisting of fine to medium sand and is the result of nearshore sedimentation processes. Longshore bars are common

on micro-tidal sandy beaches, and are characterized by a steep slope facing the beach and a smoother, longer, offshore-facing slope (Guillén and Palanques, 1993; Zhang et al., 2011). The stability and position of longshore bars are influenced by coastal dynamics such as wave energy and sea level variations. Sea level rises cause a higher wave energy and an upwards movement (Wright and Short, 1984; Lippmann and Holman, 1990). In exchange, the shape of the longshore bar controls the amount of energy that reaches the beachface and thus controls sediment erosion or accumulation. Preserved mid-Holocene peat deposits (6,725 ± 87 cal yr BP) at the base of the longshore bar (C3.1) archive information about associated paleo-landscapes, pre-existing floodplains, habitat migration, sediment stability and its seasonal equilibrium morphology (Gerdes et al., 2003; Westley and Dix, 2006; Plets et al., 2007). The sub-marine extension and formation time of the peat deposits is discussed in the following section.

Sub-marine Extension of the Peat Deposits

Corresponding to the geometry of the till deposits in the study area, peat deposits in the northern part are located in more shallow depths of ∼1 m bsl (cores B4 and B5, **Figure 2**). As these peat deposits are observed at the beach face ("observed peat" in **Figure 1**) they become increasingly exposed to coastal dynamics. Ongoing peat erosion near Lake Heiligensee (**Figure 1**) caused by a washover event was reported in spring 1995 (Krüger, 1995), and minor erosion can be observed regularly after storm surges, when peat blocks with dimensions of several decimeters are washed up on the beach. The offshore continuation of the peat layer is limited, as no corresponding deposits have been found in core C5. Peat deposits might extend below the longshore bar, as a corresponding reflector below its base (**Figure 5B**) shows similar acoustic characteristics to reflections ground truthed near core C3. A former sub-marine extension of the peat layer in the northern part of the study area is further supported by core C5. The core contains alternating layers of minerogenic lake sediments and fine sand, with a corresponding sediment sequence found below the peat deposits in core B4 (Gerdes et al., 2003).

Peat deposits in the southern and central part of the study site are better preserved due to their deeper burial (**Figure 2**). The elevation difference between the peat base in B9 in the south and in B4 in the north is ∼2 m. The southern peat deposits could be sampled both on- and offshore. Due to a comparable age of formation (discussed in section Formation Time and Local Sea Level Rise), the same sediment sequences of silty fine sand, gyttja and peat (**Figure 7**) with similar depths of these layers both on- and offshore, and corresponding horizontal reflections in the seismic data, the sub-marine peat is interpreted as a seaward extension of the peat deposits on land (**Figure 7**). Seismic data imply a seaward extension of the peat layer that was detected in C3 to the seaward dipping base of the longshore sand bar (**Figures 5C,D**), with no indication of peat deposits underneath the offshore sand ridges (core C1). Peat burial depth and thickness declines again toward south-west, and peat deposits are absent in core B7 (**Figure 2**). Onshore, peat sediments re-appear in sediment core Ig Fsb -/1956 (**Figure 1**) further south, containing peat deposits of 85 cm thickness. The reason for the hiatus found in the vicinity of B7 is most likely a single large storm surge in 1954, which eroded the covering sand layer and caused washover and erosion of peat blocks across a length of 100 m (Kolp, 1957). The sub-sedimentary, areal continuation of peat deposits under the nearshore sandbar can be roughly defined by the seismic data (**Figures 5B–D**), indicating spatial offshore extensions in the central and field observations along the northern part of the study site. Assuming a continuous deposit of the peat along the shoreline and homogeneous offshore extension, limited by the seaward extension of the longshore sand bar, a coherent submerged area of 0.16–0.2 km^2 can be estimated.

Formation Time and Local Sea Level Rise

The onset of the Heiligensee and Hütelmoor peatland formation was ascribed to Atlantic period in 5,400 yr BP (Bohne and Bohne, 2008). Submerged peat detritus (basal organic/gyttja) sampled in this study shows that the peatland development started as early as 7,024 ± 73 cal yr BP (sample C3.2). Albeit not dated, due to their base situated at 1 m bsl, peat deposits in the northern part of the study area are presumed to be younger compared to the dated peat deposits situated at a depth around 3 m bsl. An earlier formation of the peatland during the early Littorina transgression may be possible, with indications by the organic-rich layer retrieved in core C.1, but is rather unlikely. Despite the fact that the material was certainly reworked due to widely differing ages (**Figure 6**), the measured C/N ratios (11.97), $\delta^{13}C$ isotope values (−25.2‰) and the observation of marine shell fragments of the bulk material support the assumption that the increase of organic carbon content (C_{org} from 0.6 to 5.1%) within the organic layer of C1 is of marine-derived matter (Stein, 1991).

Near the shoreline, submerged gyttja deposits are overlain by peat layers dated to 6,725 ± 87 cal yr BP (C3.1). The variable presence of the gyttja—a lake sediment—is attributed to its formation in local depressions. The Hütelmoor is generally classified as a paludification mire, which formed as a consequence of a rising groundwater. However, at the same time, depressions turned into lakes within the wetland, where lacustrine sediments were deposited, and which were eventually filled up with peat by terrestrialization. The silty and clayey sediments found underneath the gyttja in the northern part of the beach are interpreted as clastic lacustrine or fluvio lacustrine sediments due to their high content of silt or clay and their position between the basin sand and the gyttja. A continuous basal sediment sequence in C3 suggests the autochthonous formation of the sediments, showing sand deposited under freshwater conditions, followed by gyttja deposited during wetland conditions and peat accumulation during the Littorina transgression. Basal peat deposits are frequently used to constrain past sea levels (Lampe and Janke, 2004; Rößler et al., 2011; Heinrich et al., 2017). In principle, the available ^{14}C ages agree with and support the local Fischland and North Rügen Holocene sea level rise curves (**Figure 6**) established by Lampe et al. (2010), but with a slight tendency toward lower sea level as determined by samples B6.1 and B6.2. The observed trend of lower reconstructed sea levels from the north (North of Rügen) to the south (this study) agrees well with different isostatic uplift rates (Lampe, 2005), with the North of Rügen experiencing uplift, and the more south Hütelmoor subsiding along the isostatic equilibrium line.

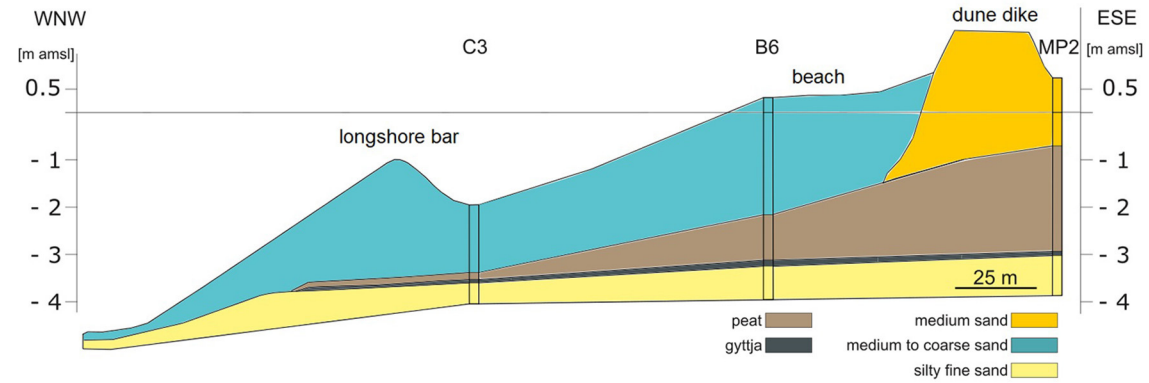

FIGURE 7 | Geological profile perpendicular to the coast with drilling locations (MP2, B6, C3—compare **Figure 1** for core locations) with sediment depths in m amsl. The information of sub-sedimentary peat continuation is based on ground truthing with core C3 and the continuation of internal reflectors in the seismic profiles.

The sharp and erosional upper boundary of both on- and offshore peat sediments indicates a sudden flooding of the former peatland. According to Meyers (1997) a C/N ratio of 20 or higher indicates terrigenous organic material and is evident within the submerged peat (C/N = 21.3 in 147 cm and 36.4 in 157 cm). In addition, a sudden increase of mean $\delta^{13}C$ isotope values from -27.9 ± 0.95 in the peat and sand deposits below the erosive boundary to -24.3 ± 0.8 in marine sands above suggests a shift from a terrestrial, freshwater environment to a marine saltwater environment (Bickert, 2000). Under the assumption of a coherent peatland system, the former erosion event of the palaeo-landscape can be constrained to a maximum age of 3,516 ± 87 cal yr BP (B6.1) and indicates a subsequent formation of the coastal longshore bar. Thereafter, the erosion of the sub-marine basal peat deposits was largely dependent on the position and stability of the longshore bar. The time frame and depth of the sampled peat deposits coincide with a period of continuously decreasing sea level rise (from >0.1 cm yr^{-1} to 0.05–0.08 cm yr^{-1}) starting around 7000 BP, allowing peat formation (~0.05–0.13 cm yr^{-1}) to keep up with the rising water table (van der Linden et al., 2008; Lampe et al., 2010, 2011). The center of the peatland was relocated from the present offshore area to the current location of the Hütelmoor. This is confirmed by peat detritus and peat of similar thickness deposited above on- and offshore basin sands in B6.2 (5,918 ± 45 cal BP), B9 (6,769 ± 128 cal BP), and C3.2 at a similar depth, respectively.

CONCLUSION

The combination of geological, geochemical and geophysical data provide a powerful method to reconstruct the coherent formation and former extension of the peatland in the working area, with peat deposits being now found across the on-/offshore zone. Slightly different formation ages are controlled by morphological differences. The large scale spatial distribution of the Hütelmoor peatland deposits since ~7,000 cal yr BP is controlled by the accommodation space above the glacial till substratum. The present offshore extension of the peat deposits is limited to the seaward base of the shore parallel sandbar. The formation of the peatland coincides with a slowdown of the sea level rise around ~7,000 cal yr BP, starting with the deposition of basal gyttja at 7,024 ± 73 cal yr BP and the deposition of peat at 6,725 ± 87 cal yr BP. As a function of coastline stability, erosion and flooding of the peatland have led and will lead to submergence of former terrestrial, high-organic material, shifting from terrestrial to marine ecosystems. It can be assumed that submerged peat layers are also present in front of other coastal peatlands along the southern Baltic Sea coast.

AUTHOR CONTRIBUTIONS

MK wrote the manuscript and conducted the geological offshore surveys. MI worked on the geological profiles, wrote the onshore descriptions and greatly supported the discussion. MJ greatly supported the research and writing of all sections of the manuscript. GR and MV supported the research and contributed to the writing of the manuscript. MN supported the geological offshore surveys and discussion on Holocene development. PF recorded hydroacoustic data and wrote the manuscript.

ACKNOWLEDGMENTS

This study was conducted within the framework of the Research Training Group Baltic TRANSCOAST funded by the DFG (Deutsche Forschungsgemeinschaft) under grant number GRK 2000/1. This is Baltic TRANSCOAST publication no. GRK2000/0012. We thank our colleagues from the GRK Baltic TRANSCOAST as well as Iris Liskow (IOW), who carried out high-quality geochemical analyses. We are grateful to Sebastian Lorenz and Jürgen Becker (University Greifswald) for support with the BOREAS-platform and the IOW-crews of the research vessels Klaashahn and Elisabeth Mann Borgese, the IOW-Scientific Divers and the support by the trainees Caroline Coccoli, Isabelle Wittstock, Florian Schneider, and Charlotte Westhoven. Further, we thank the Landesamt für Umwelt, Naturschutz und Geologie MV (LUNG) for providing detailed core data.

REFERENCES

Bickert, T. (2000). "Influence of geochemical processes on stable isotope distribution in marine sediments," in *Marine Geochemistry*, eds H. D. Schulz and M. Zabel, (Berlin; Heidelberg: Springer), 309–333.

Björck, S. (1995). A review of the history of the Baltic Sea, 13.0-8.0 ka BP. *Q. Int.* 27, 19–40. doi: 10.1016/1040-6182(94)00057-C

Bohne, B., and Bohne, K. (2008). *Monitoring zum Wasserhaushalt einer auf litoralem Versumpfungsmoor gewachsenen Regenmoorkalotte—Beispiel Naturschutzgebiet "Hütelmoor" bei Rostock*. Berlin: Aspekte der Geoökologie;Weißensee Verlag.

Caress, D. W., and Chayes, D. N. (1995). "New software for processing sidescan data from sidescan-capable multibeam sonars," in *Proceedings of the IEEE Oceans* 95 *Conference* (San Diego, CA), 997–1000.

Dahms, P. (1991). *Studie Wasserregulierung Hütelmoor*. Rostock: Unveröffentlichte Studie des StAUN Rostock.

Dietrich, R., and Liebsch, G. (2000). Zur variabilität des meeresspiegels an der küste von mecklenburg-vorpommern. *Z. Geol. Wiss.* 28, 615–624.

Feldens, P., Diesing, M., Schwarzer, K., Heinrich, C., and Schlenz, B. (2015). Occurrence of flow parallel and flow transverse bedforms in Fehmarn Belt (SW Baltic Sea) related to the local palaeomorphology. *Geomorphology* 231, 53–62. doi: 10.1016/j.geomorph.2014.11.021

Furmanczyk, K., and Dudzinska-Nowak, J. (2009). Effects of extreme storms on coastline changes: a southern Baltic example. *J. Coast. Res.* 1637–1640.

Gehrels, W. R., and Anderson, W. P. (2014). Reconstructing Holocene sea-level change from coastal freshwater peat: a combined empirical and model-based approach. *Mar. Geol.* 353, 140–152. doi: 10.1016/j.margeo.2014.04.004

Gerdes, G., Petzelberger, B. E. M., Scholz-Böttcher, B. M., and Streif, H. (2003). The record of climatic change in the geological archives of shallow marine, coastal, and adjacent lowland areas of Northern Germany. *Q. Sci. Rev.* 22, 101–124.

Guillén, J., and Palanques, A. (1993). Longshore bar and trough systems in a microtidal, storm-wave dominated coast: the Ebro Delta (Northwestern Mediterranean). *Mar. Geol.* 115, 239–252. doi: 10.1016/0025-3227(93)90053-X

Harff, J., Graf, G., and Bobertz, B. (2009). Dynamics of natural and anthropogenic sedimentation (DYNAS). *J. Mar. Sys.* 75, 315–316. doi: 10.1016/j.jmarsys.2008.04.008

Heinrich, C., Anders, S., and Schwarzer, K. (2017). Late Pleistocene and early Holocene drainage events in the eastern Fehmarn Belt and Mecklenburg Bight, SW Baltic Sea. *Boreas* 47, 754–767. doi: 10.1111/bor.12298

Koebsch, F. (2013). Dynamics of CH4 and CO_2 exchange in a Brackish Fen. *Q. Sci. Rev.* 22, 101–124.

Kolp, O. (1957). *Die Nordöstliche Heide Mecklenburgs*. Berlin: VEB Deutscher Verlag Der Wissenschaften.

Kolp, O. (1990). The Ancylus lake phase of the post-glacial evolution of the Baltic Sea. *Quaest. Geograph.*13, 69–86.

Köster, R. (1961). Junge eustatische und tektonische Vorgänge im Küstenraum der südwestlichen Ostsee. *Meyniana* 11, 23–81.

Krüger (1995). *Untersuchung zur Salzbeeinflussung überflutungsgefährdeter, forstlich genutzter Flächen im Naturschutzgebiet Hütelmoor-Heiligensee.* Rostock: Dipliomarbeit am Fachbereich Landeskultur und Umweltschutz der Universität Rostock.

Lampe, R. (2002). *Holocene Evolution of the South-Western Baltic Coast: Geological, Archaeological and Palaeo-Environmental Aspects: Field Meeting of INQUA Subcommission V Sea-Level Changes and Coastal Evolution, Western Europe, Western Europe, September 22-27, (2002)*. Greifswald: Ernst-Moritz-Arndt-Universität.

Lampe, R. (2005). Lateglacial and Holocene water-level variations along the NE German Baltic Sea coast: review and new results. *Q. Int.* 133–134, 121–136. doi: 10.1016/j.quaint.2004.10.005

Lampe, R., Endtmann, E., Janke, W., and Meyer, H. (2010). Relative sea-level development and isostasy along the NE German Baltic Sea coast during the past 9 ka. *E&G Q. Sci. J.* 59, 3–20. doi: 10.3285/eg.59.1-2.01

Lampe, R., and Janke, W. (2004). The Holocene sea level rise in the Southern Baltic as reflected in coastal peat sequences. *Polish Geol. Ins. Spec. Pap.* 11, 19–30.

Lampe, R., Lorenz, S., Janke, W., Meyer, H., Küster, M., Hübener, T., et al. (2009). *Zur Landschafts- und Gewässergeschichte der Müritz: Umweltgeschichtlich Orientierte Bohrungen 2004 - 2006 Zur Rekonstruktion der Nacheiszeitlichen Entwicklung*. Greifswald: Geozon Science Media.

Lampe, R., Naumann, M., Meyer, H., Janke, W., and Ziekur, R. (2011). "Holocene evolution of the southern baltic sea coast and interplay of sea-level variation, isostasy, accommodation and sediment supply," in *The Baltic Sea Basin, Central and Eastern European Development Studies (CEEDES)*, eds J. Harff, S. Björck, and P. Hoth (Berlin; Heidelberg: Springer), 233–251.

Lehfeldt, R., and Milbradt, P. (2000). "Longshore sediment transport modeling in 1 and 2 dimensions, in: advances in Hydro-science and engineering," in *Proceedings of the 4th International Conference on Hydro-Science and Engineering Abstract* (Seoul).

Lemke, W. (1998). Sedimentation und paläogeographische Entwicklung im westlichen Ostseeraum (Mecklenburger Bucht bis Arkonabecken) vom Ende der Weichselvereisung bis zur Litorinatransgression. *Meereswissenschaftliche Berichte* 31, 156.

Lippmann, T. C., and Holman, R. A. (1990). The spatial and temporal variability of sand bar morphology. *J. Geophys. Res.* 95:11575. doi: 10.1029/JC095iC07p11575

Meyers, P. A. (1997). Organic geochemical proxies of paleoceanographic, paleolimnologic, and paleoclimatic processes. *Org. Geochem.* 27, 213–250. doi: 10.1016/S0146-6380(97)00049-1

Miegel, K., Graeff, T., Selle, B., Salzmann, T., Franck, C., and Bronstert, A. (2016). Untersuchung eines renaturierten Niedermoores an der mecklenburgischen Ostseeküste - Teil I: Systembeschreibung und hydrologische Grundcharakterisierung (Investigation of a renatured fen on the Baltic Sea coast of Mecklenburg - Part I: system description and basic hydrological characterisation). *Hydrol. Wasserbew.* 60, 242–258. doi: 10.5675/HyWa_2016,4_1

Milliman, J. D., and Emery, K. O. (1968). Sea levels during the past 35,000 years. *Science* 162, 1121–1123. doi: 10.1126/science.162.3858.1121

Nicholls, R. J., and Cazenave, A. (2010). Sea-level rise and its impact on coastal zones. *Science* 328, 1517–1520. doi: 10.1126/science.1185782

Nieuwenhuize, J., Maas, Y. E. M., and Middelburg, J. J. (1994). Rapid analysis of organic carbon and nitrogen in particulate materials. *Mar. Chem.* 45, 217–224. doi: 10.1016/0304-4203(94)90005-1

Nnafie, A., de Swart, H. E., Calvete, D., and Garnier, R. (2014). Effects of sea level rise on the formation and drowning of shoreface-connected sand ridges, a model study. *Cont. Shelf Res.* 80, 32–48. doi: 10.1016/j.csr.2014.02.017

Pendleton, E. A., Brothers, L. L., Thieler, E. R., and Sweeney, E. M. (2017). Sand ridge morphology and bedform migration patterns derived from bathymetry and backscatter on the inner-continental shelf offshore of Assateague Island, USA. *Cont. Shelf Res.* 144, 80–97. doi: 10.1016/j.csr.2017.06.021

Plets, R., Dix, J., Bastos, A., and Best, A. (2007). Characterization of Buried inundated Peat on Seismic (Chirp) data, inferred from core information. *Archaeol. Prospection* 14, 261–272. doi: 10.1002/arp.318

Rebentrost, G. (1973). *Beschreibung von Rückgangserscheinungen der Rostocker Heide in den Letzten Jahren auf der Strecke Uhlenflucht bis Stromgrabenmündung*. Rostock: Akademie der Wissenschaften der DDR, Institut für Meereskunde Warnemünde.

Reimann, T., Tsukamoto, S., Naumann, M., and Frechen, M. (2011). The potential of using K-rich feldspars for optical dating of young coastal sediments-A test case from Darss-Zingst peninsula (southern Baltic Sea coast). *Q. Geochronol.* 6, 207–222. doi: 10.1016/j.quageo.2010.10.001

Reimer, P. J., Bard, E., Bayliss, A., Warren, B. J., Blackwell, P. G., Ramsey, C. B., et al. (2013). Intcal13 and marine13 radiocarbon age calibration curves 0–50,000 years cal bp. *Radiocarbon* 55, 1869–1887. doi: 10.2458/azu_js_rc.55.16947

Rosentau, R., Meyer, M., Harff, J., Dietrich, R., and Richter, A. (2007). Relative sea level change in the Baltic Sea since the Littorina Transgression. *Z. Geol. Wiss.* 35, 3–16.

Rößler, D., Moros, M., and Lemke, W. (2011). The Littorina transgression in the southwestern Baltic Sea: new insights based on proxy methods and radiocarbon dating of sediment cores. *Boreas* 40, 231–241. doi: 10.1111/j.1502-3885.2010.00180.x

Schlungbaum, G., and Voigt, B. (2001). "Die Darß-Zingster Bodden-ein junges Gewässersystem in einer noch nicht alten Landschaft,"in *Die Darß-Zingster Bodden. Monographie Einer Einzigartigen Küstenlandschaft*. (Stralsund: Meer und Museum), 5–16.

Schwarzer, K. (2010). Aggregate resources and extraction in the baltic sea: an introduction. *J. Coast. Res.* 165–172.

Small, C., and Nicholls, R. J. (2003). A global analysis of human settlement in coastal zones. *J. Coast. Res.* 19, 584–599. doi: 10.2307/4299200

Snedden, J. W., and Dalrymple, R. W. (1999). Modern shelf sand ridges: from historical perspective to a unified hydrodynamic and evolutionary model. *Soc. Sediment. Geol.* 64, 13–28.

Stein, R. (1991). "Accumulation of organic carbon in Baffin Bay and Labrador Sea sediments (ODP-Leg 105)," in *Accumulation of Organic Carbon in Marine Sediments: Results from the Deep Sea Drilling Project/Ocean Drilling Program* (DSDP/ODP) (Berlin Heidelberg: Springer), 40–84.

Sterr, H. (2008). Assessment of vulnerability and adaptation to sea-level rise for the coastal zone of germany. *J. Coast. Res.* 24, 380–393. doi: 10.2112/07A-0011.1

Stigge, H. J., Weiss, D., Biermann, S., Weigt, R., Redieck, M., and Schade, A. (2005). *Dokumentation der Sturmflut vom 3. und 4. November 1995 an der Küste von Mecklenburg Vorpommern* (Schwerin: Verlag Rediecke & Schade GmbH), 17–20.

Swift, D. J. P., Parker, G., Lanfredi, N. W., Perillo, G., and Figge, K. (1978). Shoreface-connected sand ridges on american and european shelves: a comparison. *Estuarine Coast. Mar. Sci.* 7, 257–273. doi: 10.1016/0302-3524(78)90109-3

Thorne, C., Evans, E., and Penning-Rowsell, E. (2007). *Future Flooding and Coastal Erosion Risks*. London: Thomas Telford, p350.

Valiela, I. (2009). *Global Coastal Change*. Hoboken, NJ: John Wiley & Sons.

van de Meene, J. W. H., and van Rijn, L. C. (2000). The shoreface-connected ridges along the central Dutch coast—part 1: field observations. *Cont. Shelf Res.* 20, 2295–2323. doi: 10.1016/S0278-4343(00)00048-0

van der Linden, M., Barke, J., Vickery, E., Charman, D. J., and van Geel, B. (2008). Late holocene human impact and climate change recorded in a north swedish peat deposit. *Palaeogeogr. Palaeoclimatol. Palaeoecol.* 258, 1–27. doi: 10.1016/j.palaeo.2007.11.006

Vestergaard, P. (1997). Possible impact of sea-level rise on some habitat types at the Baltic coast of Denmark. *J. Coast. Conserv.* 3, 103. doi: 10.1007/BF02908185

Voigtländer, U., Schmidt, J., and Scheller, W. (1996). *Pflege-und Entwicklungsplan NSG*. Schwerin: Heiligensee und Hütelmoor.

Westley, K., and Dix, J. (2006). Coastal environments and their role in prehistoric migrations. *J. Marit. Archaeol.* 1, 9–28. doi: 10.1007%2Fs11457-005-9004-5

Wong, P. P., Losada, I. J., Gattuso, J.-P., Hinkel, J., Khattabi, A., McInnes, K. L., et al. (2014). Coastal systems and low-lying areas. *Clim. Change* 2104, 361–409. doi: 10.1017/CBO9781107415379.010

Wright, L. D., and Short, A. D. (1984). Morphodynamic variability of surf zones and beaches: a synthesis. *Mar. Geol.* 56, 93–118. doi: 10.1016/0025-3227(84)90008-2

Zeiler, M., Schwarzer, K., and Ricklefs, K. (2008). Seabed morphology and sediment dynamics. *Die Küste* 74, 31–44.

Zhang, W., Harff, J., and Schneider, R. (2011). Analysis of 50-year wind data of the southern Baltic Sea for modelling coastal morphological evolution – a case study from the Darss-Zingst Peninsula. *Oceanologia* 53, 489–518. doi: 10.5697/oc.53-1-TI.489

Conflict of Interest Statement: The authors declare that the research was conducted in the absence of any commercial or financial relationships that could be construed as a potential conflict of interest.